

The energy spectra of heavy nuclei measured by the ATIC experiment

A. D. Panov ^{a,*}, J. H. Adams Jr ^b, H. S. Ahn ^c,
G. L. Bashindzhagyan ^a, K. E. Batkov ^a, J. Chang ^{d,g},
M. Christl ^b, A. R. Fazely ^e, O. Ganel ^c, R. M. Gunasingha ^e,
T. G. Guzik ^f, J. Isbert ^f, K. C. Kim ^c, E. N. Kouznetsov ^a,
M. I. Panasyuk ^a, W. K. H. Schmidt ^d, E. S. Seo ^c,
N. V. Sokolskaya ^a, J. P. Wefel ^f, J. Wu ^c, V. I. Zatsepin ^a

^a*Skobeltsyn Institute of Nuclear Physics, Moscow State University, Russia*

^b*Marshall Space Flight Center, Huntsville, AL, USA*

^c*University of Maryland, College Park, MD, USA*

^d*Max Planck Institute fur Aeronomie, Lindau, Germany*

^e*Southern University, Baton Rouge, LA, USA*

^f*Louisiana State University, Baton Rouge, LA, USA*

^g*Purple Mountain Observatory, Chinese Academy of Science, Nanjing, China*

Abstract

The preliminary energy spectra of heavy nuclei C, O, Ne, Mg, Si, and Fe in the primary cosmic rays measured by the ATIC-2 experiment are presented and compared to previous data and to propagation models. The ATIC results are consistent with a simple leaky box model propagation, but a modified leaky box gives a better fit. Using previous data to extend the ATIC-2 results for all heavy nuclei to higher energy, the combined spectra can be best fit with a modified leaky box model or a compound diffusion model with a Kolmogorov spectrum of magnetic field fluctuations becoming dominant at high energy.

Key words: Cosmic rays, Heavy nuclei, Energy spectra, Propagation models
PACS: 96.40.De, 95.55.Vj, 29.40.Wk

* Corresponding author

1 Introduction

ATIC (Advanced Thin Ionization Calorimeter) is a balloon borne experiment designed to measure cosmic ray composition for elements from hydrogen to iron and their energy spectra from 50 GeV to near 100 TeV. ATIC had two successful balloon flights in Antarctica: from 28 Dec 2000 to 13 Jan 2001 (test flight ATIC-1) and from 29 Dec 2002 to 18 Jan 2003 (science flight ATIC-2).

ATIC is comprised of a fully active bismuth germanate (BGO) calorimeter, a carbon target with embedded scintillator hodoscopes, and a silicon matrix that is used as a charge detector in the experiment (see Fig. 1). The detailed description of the ATIC spectrometer, and the method of calorimeter calibration may be found in [1]. The description of the silicon matrix charge detector is given in [2,3].

2 Charge resolution

In the experiment, the events selected are those in which a primary particle passes through the charge module, interacts in the carbon target, and generates an electron-hadron cascade in the calorimeter. An example of reconstruction of the trajectory and measurement of the charge are shown in Fig. 2. Since the BGO crystals in alternate layers are orthogonal (see Fig 1), there are four X and four Y positions of the shower axis to be fit to determine the trajectory, which is then projected to the Si-matrix layer, as illustrated in Fig. 2.

In the ATIC-2 exposure, the charge resolution was acceptable for all elements at all energies as illustrated in Fig. 3 for the region from B to Ni. The charge resolutions for some even heavy nuclei are presented in Table 1. Charge resolutions were calculated by approximation of charge peaks by gaussians (Fig. 4). These estimations are similar to the data obtained for ATIC-1 in ref. [3]. We present here preliminary energy spectra for the heavy nuclei and compare the results to previous data and to models of cosmic ray propagation in the galaxy.

3 Conversion to primary spectrum

The energy deposit E_d in the calorimeter in each reconstructed event is determined by summing the energy deposits in all BGO crystals. To convert a spectrum in E_d to spectrum in primary energy E we adopt the approximation used in emulsion chamber calorimeter analysis [4]. A shift is used along the

energy axis by k_s^{-1} , where

$$k_s = \int_0^1 k^{\gamma+1} \times f(k) dk \Big/ \int_0^1 k^\gamma \times f(k) dk.$$

Here $f(k)$ is distribution of $k = E_d/E$ value at given E , and γ is the index of integral spectrum. The values of k_s were obtained using simulation of passing particles through ATIC with FLUKA code [5,6] for different nuclei and for spectrum with $\gamma = 1.6$. The resulting k_s values are only weakly dependent on the choice of $\gamma = 1.6$. For a constant value of k_s , the spectral index is not altered between the E_d spectrum and E spectrum. Generally, k_s values depend on E due to leakage through the bottom and sides of the calorimeter. Our preliminary estimation shows that this dependence is weak, and leads to steepening of E_d spectrum by $\Delta\gamma = 0.04$. In the present paper, spectral shapes are presented without taking into account this correction factor, which needs to be refined. The fluxes were determined by the formula:

$$I = \frac{dN}{dE} \Big/ (S\Omega \times T \times \epsilon \times \eta \times W_{eff}),$$

where $S\Omega$ is geometry factor, T is exposure live time, ϵ is efficiency of event reconstructing algorithm, η is correction factor for attenuation in the residual atmosphere, and $W_{eff} = \int_0^1 k^\gamma f(k) dk / k_s^\gamma$. These values will be presented in more detail in a future paper.

It should be noted that this technique is only a first step toward accurate solution of the deconvolution problem to obtain energy spectra of primaries from the spectra of energy deposit. Therefore the data of the present report should be considered as preliminary.

4 Results and discussion

The energy spectra (per nucleon) for abundant nuclei C, O, Ne, Mg, Si, Fe along with the data of HEAO-3-C2 experiment [7] and CRN experiment [8] are shown in Fig. 5. The agreement with the previous data is generally quite good.

To interpret the experimental spectra we use the Leaky Box approximation of the transport equation [9, pp. 119–122] to describe propagation of particles in the interstellar medium and transformation of primary spectra during propagation. The spectrum of a particle in this framework may be written as:

$$N_P(E) = \frac{Q_P(E)\tau_{esc}(R)}{1 + \lambda_{esc}(R)/\lambda_P}, \quad (1)$$

where $N_P(E)$ is the measured spectrum of particle P , $Q_P(E)$ is the spectrum at the source, R is the magnetic rigidity of the particle, $\lambda_{esc}(R)$ is the mean amount of matter traversed by a particle without nuclear fragmentation process, λ_P is the fragmentation length, and $\tau_{esc} = \lambda_{esc}/(v\rho)$. In the last formula v is the velocity of the particle and ρ is density of the interstellar medium.

In the HEAO3-C2 experiment [7] it was shown that the experimental data for energies below 35 GeV/n can be described by the Leaky Box model with a source spectrum in the shape of a power law in momentum with a spectral index 2.23, and B/C ratio data of HEAO produces the following dependency $\lambda_{esc}(R)$ [7]:

$$\begin{cases} \lambda_{esc} = 34.1\beta R^{-0.6} \text{ g cm}^{-2}, & R > 4.4\text{GV} \\ \lambda_{esc} = 14.0\beta, & R < 4.4\text{GV}. \end{cases} \quad (2)$$

The predictions of the model Eqs. (1,2) are shown as dashed lines compared to the data in Fig. 5. The agreement is acceptable, but the dashed curves appear to underestimate the ATIC-2 data, particularly C, O, Ne and Si at the highest energies.

The power law form of λ_{esc} Eq. (2) implies a very short escape length at high energies and this would imply a larger anisotropy than has been observed [13]. To resolve this problem Swordy [14] suggested that the escape length should have a finite value as a high energy asymptote. In this approximation, Eq. (2) for $R > 4.4$ GV takes the form:

$$\lambda_{esc} = 34.1\beta R^{-0.6} + \lambda_r \text{ g cm}^{-2}. \quad (3)$$

Adopting $\lambda_r = 0.13$ in Eq. (3) yields predictions shown as the solid lines in Fig. 5. This improves the fit to the individual element spectra at highest energies but the statistics are not sufficient to make definite conclusions.

To improve the statistics at the highest energy, Fig. 6 shows a plot of all nuclei heavier than Boron, as a function of energy per particle. The ATIC-2 results are compared to the data from JACEE [10], MUBEE [11], and SOKOL [12]. The ATIC-2 results are in good agreement with the SOKOL results below 30 TeV and definitely point out to deviation from the simple Leaky Box model and to better agreement with the model Eqs. (1,3). In the energy range higher than 30 TeV the statistics of the ATIC data are too poor to make choice between the simple Leaky Box model and the Swordy model. However, it is visible that simple Leaky Box model with power law for λ_{esc} as in Eqs. (1,2) falls below other experimental data at the highest energies.

Turning next to the diffusion model, a problem has persisted for many years

between the apparent energy dependence as given in Eq. (2) and the expected form derived from the Kolmogorov spectrum of magnetic field fluctuations which predicts an escape length proportional to rigidity to the $-1/3$ power [15,16]. The steeper dependence found experimentally, at lower energies, has been attributed to both reacceleration during propagation and to the damping of the magnetic field fluctuations by the cosmic rays themselves [16]. In such a model, the escape length is expected to evolve with energy into the Kolmogorov dependence at high energy where reacceleration and wave damping become unimportant. A representation of this model is shown by the dotted line in Fig. 6, where the $R^{-1/3}$ form was assumed for λ_{esc} above 10 TeV.

5 Conclusions

The ATIC-2 results on the spectra of heavy nuclei are in agreement with previous data from HEAO and CRN and Sokol. The results can be explained with the leaky box model with the addition of a high energy asymptote to the escape length giving a better fit to the overall dataset. Viewed from the perspective of the diffusion model, the results suggest that there may be differences in the propagation of the cosmic rays at different energies. The ATIC results are still preliminary and further analysis is underway, as is the prospect of a re-flight of the instrument to further improve the results.

Acknowledgements

The work was supported by Russian Foundation for Basic Research grants Nos. 99-02-16246 and 02-02-1645 in Russia, NASA grants Nos. NAG5-5064, NAG5-5306, NAG5-5155, NAG5-5308 and the NASA SR&T program in the USA, and the Chinese Academy of Sciences and the Max-Planck Institute.

References

- [1] T. G. Guzik, J. H. Adams, H. S. Ahn, et al. (ATIC Collaboration), The ATIC long duration balloon project, *Adv. Sp. Res.* **33** (10) (2004) 1763–1770.
- [2] J. H. Adams, G. L. Bashindzhagyan, V. I. Zatsepin, M. M. Merkin, M. I. Panasyuk, G. A. Samsonov, N. V. Sokol'skya, L. A. Khein, The silicon matrix as a charge detector for the ATIC experiment, *Instruments and Experimental Techniques* **44** (4) (2001) 455–461.

- [3] V. I. Zatsepin, J. H. Adams, H. S. Ahn, et al. (ATIC Collaboration), The silicon matrix as a charge detector in the ATIC experiment, *Nucl. Instr. Meth. A* 524 (2004) 195–207.
- [4] T. H. Burnett, S. Dake, M. Fuki, et al. (JACEE Collaboration), Jacee emulsion chambers for studying the energy spectra of high energy cosmic ray protons and helium, *Nucl. Instr. Meth. A* 251 (1986) 583–595.
- [5] A. Fassó, A. Ferrari, P.R. Sala, Electron-photon transport in FLUKA: status, in: A. Kling, F. Barao, M. Nakagawa, L. Tavora, P. Vaz (Eds.), *Proceedings of the MonteCarlo 2000 Conference*, Lisbon, October 23–26 2000, Springer-Verlag, Berlin, 2001, pp. 159–164.
- [6] A. Fassó, A. Ferrari, J. Ranft, P.R. Sala, FLUKA: Status and prospective for hadronic applications, in: A. Kling, F. Barao, M. Nakagawa, L. Tavora, P. Vaz (Eds.), *Proceedings of the MonteCarlo 2000 Conference*, Lisbon, October 23–26 2000, Springer-Verlag, Berlin, 2001, pp. 955–960.
- [7] J. J. Engelmann, P. Ferrando, A. Soutoul, et al. (HEAO Collaboration), Charge composition and energy spectra of cosmic-ray nuclei for elements from Be to Ni. results from HEAO-3-C2, *Astron. Astrophys.* 233 (1990) 96–111.
- [8] D. Müller, S. P. Swordy, P. Meyer, J. L’Heureux, J. M. Grunsfeld, Energy spectra and composition of primary cosmic rays, *The Astrophysical Journal* 374 (1991) 356–365.
- [9] T. K. Gaisser, *Cosmic rays and particle physics*, Cambridge University Press, New York, 1990.
- [10] Y. Takahashi, et al. (JACEE Collaboration), Elemental abundance of high energy cosmic rays, *Nucl. Physics B (Proc. Suppl.)* 60B (1998) 83–92.
- [11] V. I. Zatsepin, E. A. Zamchalova, A. Y. Varkovitskaya, N. V. Sokolskaya, G. P. Sazhina, T. V. Lazareva, Energy spectra of primary protons and other nuclei in energy region 10–100 TeV/nucleus, in: *23rd ICRC*, Vol. 2, 1993, pp. 13–16.
- [12] I. P. Ivanenko, V. Y. Shestoporov, L. O. Chikova, et al., Energy spectra of cosmic rays above 2 TeV as measured by the “Sokol” apparatus, in: *23rd International Cosmic Ray Conference*, Vol. 2, Calgary, 1993, pp. 17–20.
- [13] A. D. Erlykin, M. Lipsky, A. W. Wolfendale, Hight energy cosmic ray spectroscopy. IV. The evidence from direct observation at lower energies and directional anisotropies, *Astroparticle Physics* 8 (1998) 283–292.
- [14] S. P. Swordy, Expectation for cosmic ray composition changes in the region 10^{14} to 10^{16} eV, in: *24th International Cosmic Ray Conference*, Vol. 2, 1995, pp. 697–700.
- [15] V. S. Ptuskin, Cosmic ray origin: general overview, in: M. Shapiro, T. Stanev, J. Wefel (Eds.), *Astrophysical sources of high energy particles and radiation*, Kluwer Academic Publisher, Netherlands, 2001, pp. 251–262.

- [16] V. S. Ptuskin, I. V. Moskalenko, F. C. Jones, A. W. Strong, S. G. Mashnik, Propagation model for cosmic ray species in the Galaxy, arXiv:astro-ph/0301420 (2003).

Table 1

Charge resolutions for heavy nuclei at different energies. The represented values are the standard deviations of appropriate gaussians

E_d , GeV	C	O	Ne	Mg	Si
> 50	0.29	0.29	0.31	0.34	0.35
> 250	0.26	0.28	0.29	0.34	0.34
> 1000	0.26	0.28	0.32	0.30	0.39

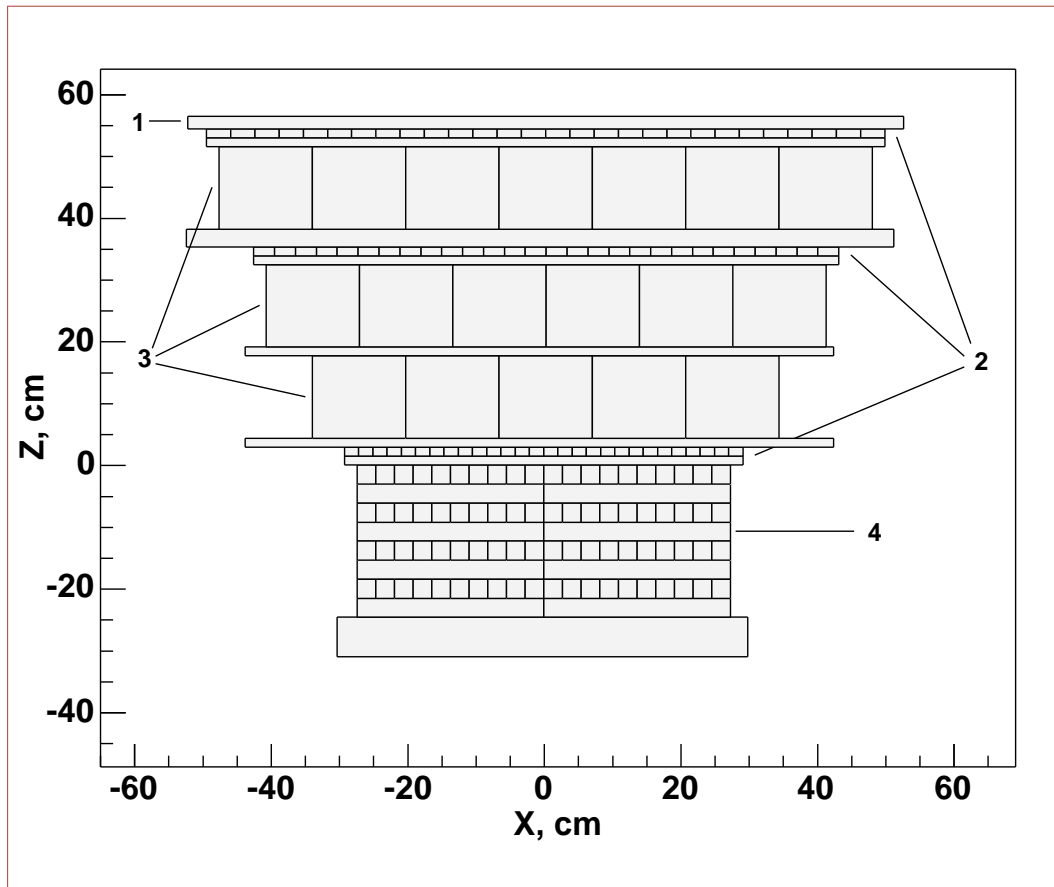


Fig. 1. Schematic view of the ATIC spectrometer: 1—silicon matrix, 2—scintillator hodoscopes, 3—carbon target, 4—BGO calorimeter.

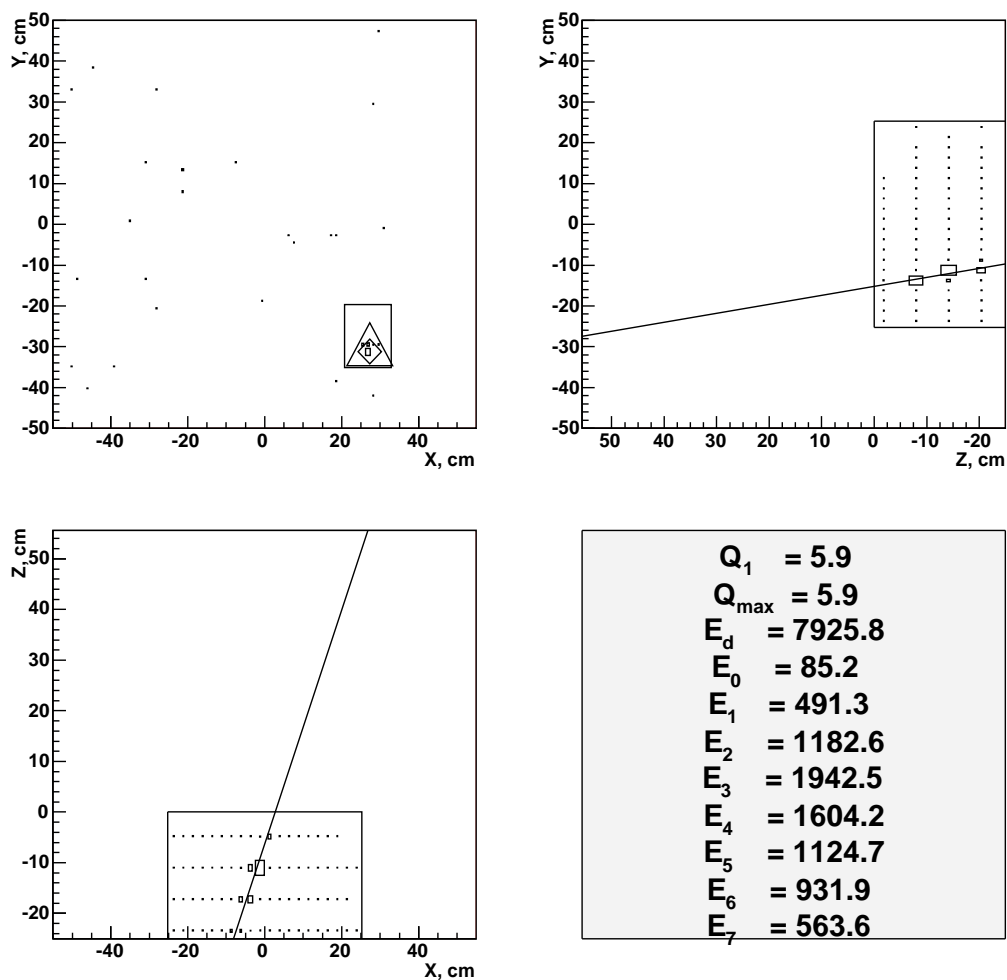


Fig. 2. An example of reconstruction of trajectory and measurement of particle charge. E_d —energy deposit in the calorimeter in GeV; Q_1 —the charge of particle that was found within the error corridor of the trajectory, Q_{\max} —the maximal charge in the whole silicon matrix (in this event Q_1 and Q_{\max} are the same); E_0 – E_7 —energy deposits (in GeV) in the each of eight layers of the calorimeter.

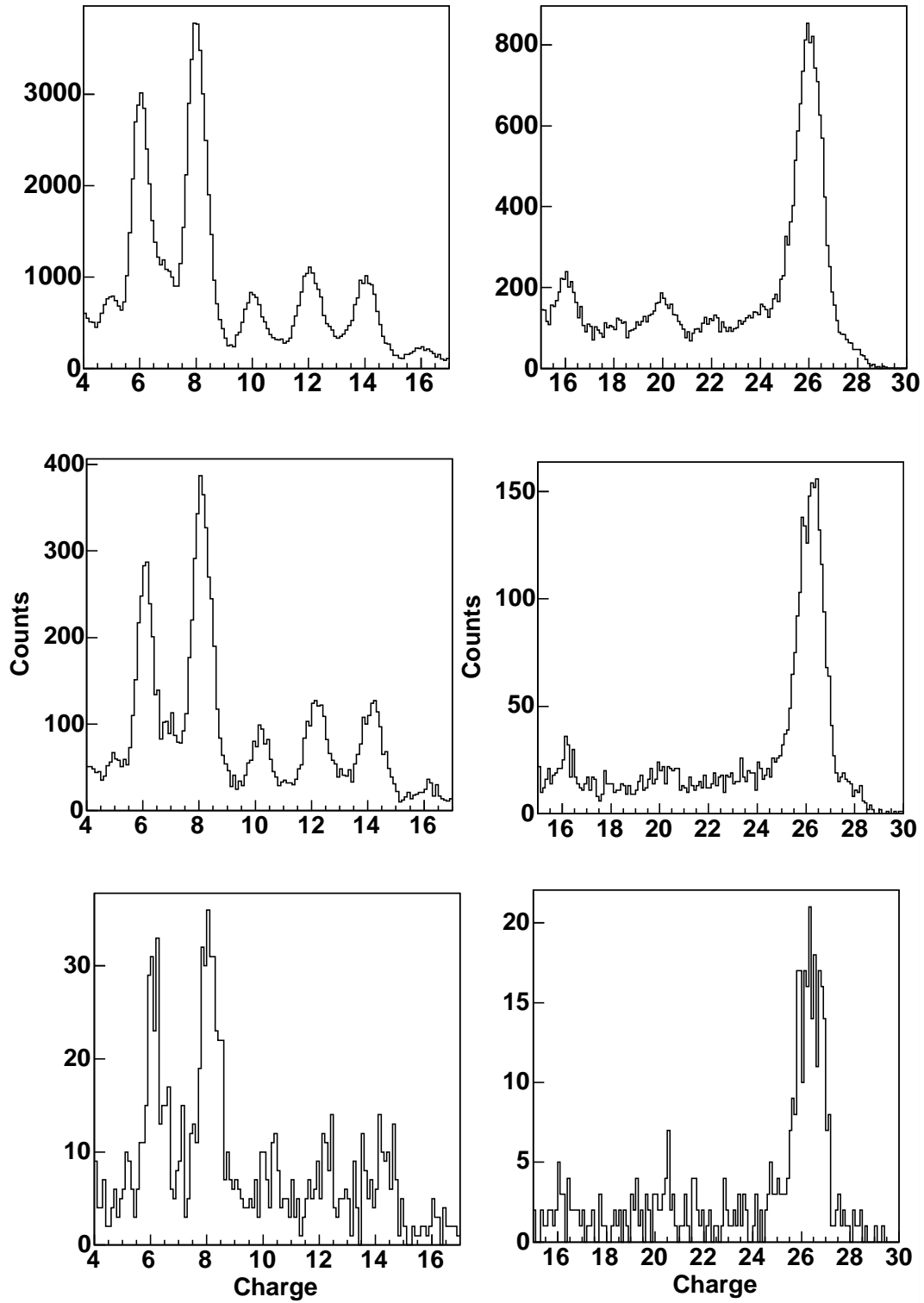


Fig. 3. Charge histograms for the heavy nuclei measured in ATIC-2 for different energy thresholds. First row is $E_d > 50$ GeV, second row is $E_d > 250$ GeV and third row is $E_d > 1000$ GeV.

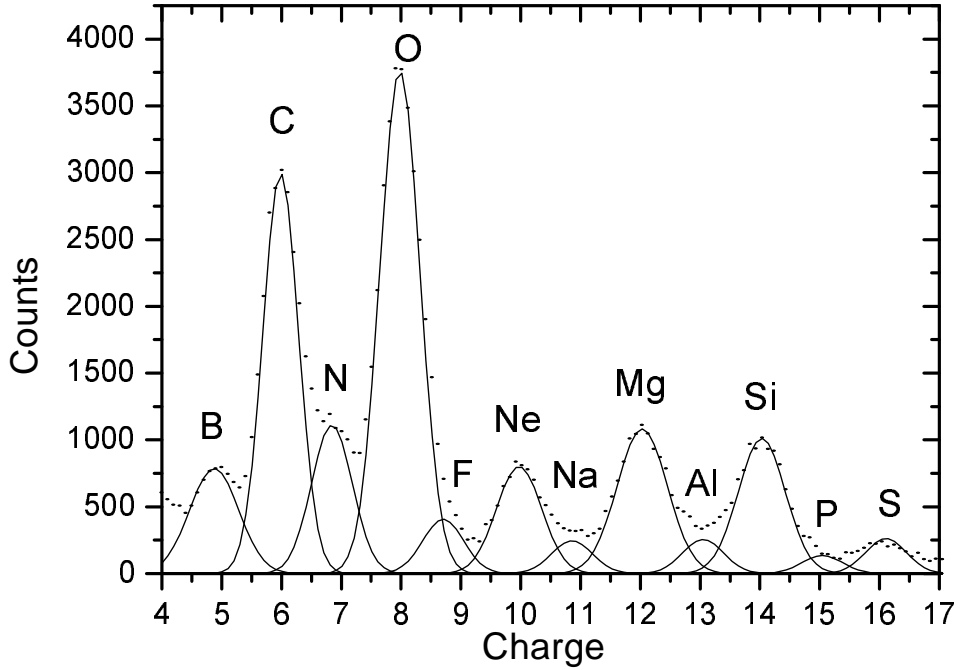


Fig. 4. Decomposition of the charge spectrum for $E_d > 50$ GeV by Gaussians.

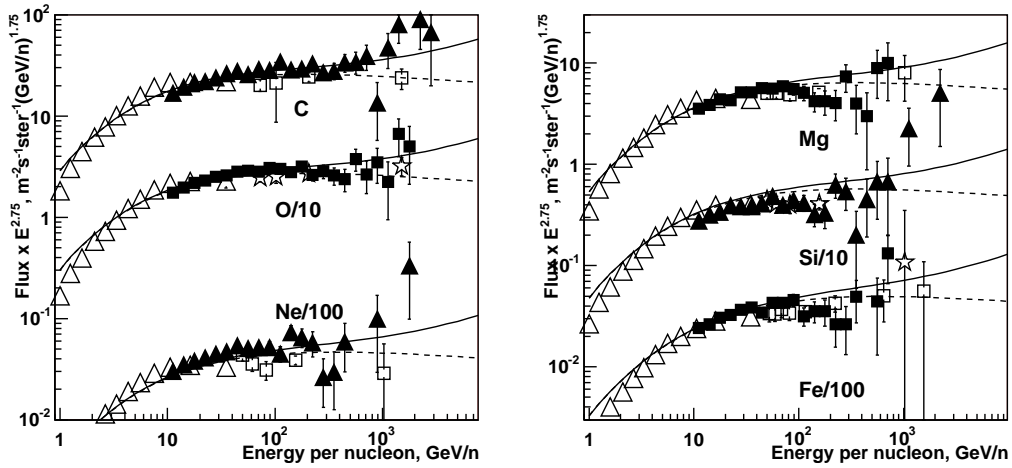


Fig. 5. Energy spectra (per nucleon) for even abundant nuclei. Open triangles or stars—the data of HEAO-3-C2 [7]; open squares—the data of CRN [8]; filled marks—data of ATIC-2. The curves show results of propagation calculations as discussed in the text.

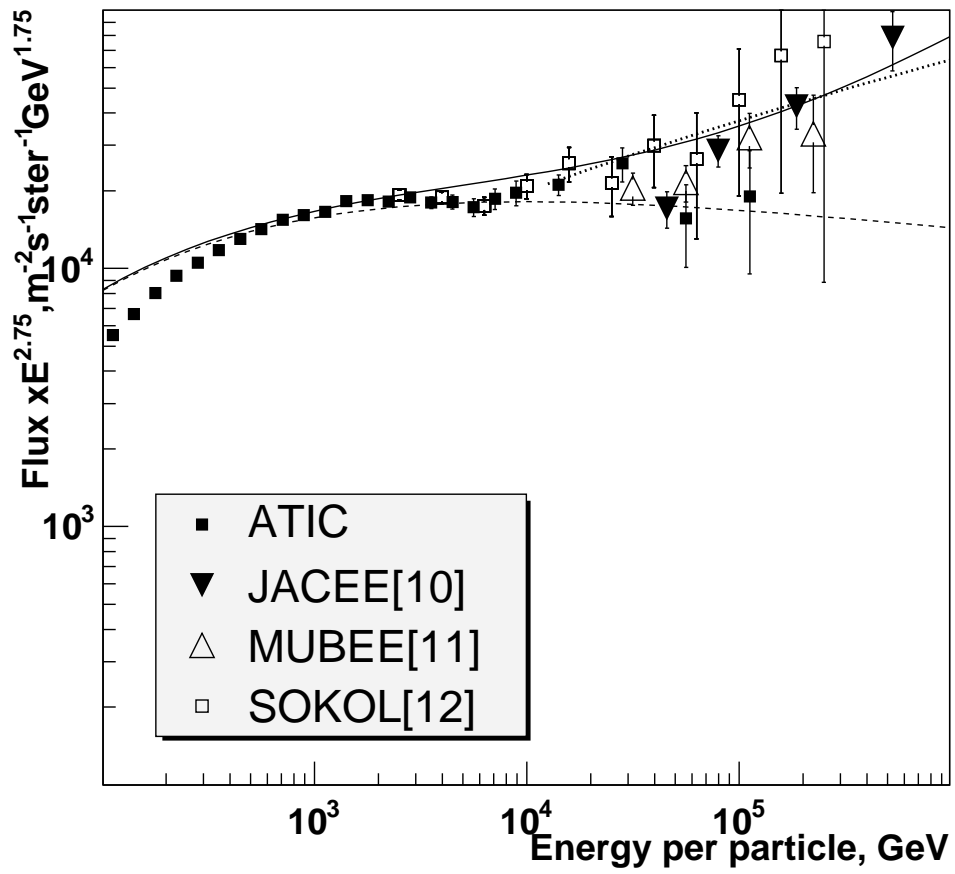


Fig. 6. Energy spectra (per particle) for all nuclei heavier the Boron. The curves show propagation model calculations as described in the text.